Clinical & Experimental Metastasis (2022) 39:815–831
https://doi.org/10.1007/s10585-022-10182-7

RESEARCH PAPER

Metastasis suppressor NME1 in exosomes or liposomes conveys motility and migration inhibition in breast cancer model systems

Imran Khan[1] · Brunilde Gril[1] · Ayuko Hoshino[2,3,4] · Howard H. Yang[5] · Maxwell P. Lee[5] · Simone Difilippantonio[6] · David C. Lyden[2,3] · Patricia S. Steeg[1]

Received: 15 April 2022 / Accepted: 27 July 2022 / Published online: 8 August 2022

Abstract

Tumor-derived exosomes have documented roles in accelerating the initiation and outgrowth of metastases, as well as in therapy resistance. Little information supports the converse, that exosomes or similar vesicles can suppress metastasis. We investigated the NME1 (Nm23-H1) metastasis suppressor as a candidate for metastasis suppression by extracellular vesicles. Exosomes derived from two cancer cell lines (MDA-MB-231T and MDA-MB-435), when transfected with the NME1 (Nm23-H1) metastasis suppressor, secreted exosomes with NME1 as the predominant constituent. These exosomes entered recipient tumor cells, altered their endocytic patterns in agreement with NME1 function, and suppressed in vitro tumor cell motility and migration compared to exosomes from control transfectants. Proteomic analysis of exosomes revealed multiple differentially expressed proteins that could exert biological functions. Therefore, we also prepared and investigated liposomes, empty or containing partially purified rNME1. rNME1 containing liposomes recapitulated the effects of exosomes from NME1 transfectants in vitro. In an experimental lung metastasis assay the median lung metastases per histologic section was 158 using control liposomes and 15 in the rNME1 liposome group, 90.5% lower than the control liposome group ($P = 0.016$). The data expand the exosome/liposome field to include metastasis suppressive functions and describe a new translational approach to prevent metastasis.

Keywords Metastasis suppressor · NME · Exosomes · Breast cancer metastasis · Liposomes

Introduction

Tumor metastasis, the process by which tumor cells leave a primary tumor to successfully colonize a distant organ, is a major contributor to cancer patients' deaths, either by direct organ compromise or side effects of its treatment [1]. Despite decades of mechanistic research, a diagnosis of metastatic cancer is usually a terminal illness. A known contributor to the metastatic process is tumor-derived exosomes, membrane-enclosed vesicles of 30–150 nm diameter, containing proteins, RNAs and other components [2–5]. In vivo, exosomes promote the development of a pre-metastatic niche, regulate tumor cell interactions with the microenvironment, promote angiogenesis, guide target organ colonization, and determine metastatic site specificity [6–13]. Exosomes also promote other clinically relevant aspects of cancer aggressiveness such as chemoresistance and immune responses [14, 15].

In contrast, only sporadic reports have investigated a potential metastasis suppressive effect of exosomes or other

✉ Imran Khan
imran.khan@nih.gov

1 Women's Malignancies Branch, Center for Cancer Research, National Cancer Institute, NIH, Building 37, Convent Drive, Room 1126, Bethesda, MD 20892, USA

2 Children's Cancer and Blood Foundation Laboratories, Departments of Pediatrics, Cell and Developmental Biology, Weill Cornell Medical College, New York, NY, USA

3 Department of Pediatrics, Memorial Sloan-Kettering Cancer Center, New York, NY, USA

4 School of Life Science and Technology, Tokyo Institute of Technology, Yokohama, Japan

5 Laboratory of Cancer Biology and Genetics, Center for Cancer Research, National Cancer Institute, NIH, Bethesda, USA

6 Laboratory Animal Sciences Program, Frederick National Laboratory for Cancer Research, National Cancer Institute, Frederick, MD, USA

membranous vesicles. In vitro experiments demonstrated inhibition of tumor migration by exosomal miRNAs [16, 17]. Mesenchymal stem cells overexpressing miR-128 produced miR-128 containing exosomes that inhibited urothelial carcinoma proliferation and invasion in vitro, and inhibited tumorigenesis and metastasis in vivo [18]. Synthetic folic acid modified exosomes containing hyaluronidase reduced murine 4T1 mammary carcinoma migration in vitro and lung metastasis in vivo [19]. If more thoroughly understood, the existence of metastasis suppressive extracellular vesicles could represent a potential new translational advance. Many issues remain in this nascent literature including the role of other protein and miRNA cargoes in the exosomes, mechanisms of action on target tumor and/or microenvironmental cells, optimal delivery doses and schedules, etc. In addition to miRNAs, the metastasis suppressor proteins stand as notable candidates for participation in such processes.

We have asked if the NME1 metastasis suppressor confers motility, migration and metastasis suppressive activity through extracellular vesicles. Metastasis suppressors are genes, RNAs and/or proteins that, when re-expressed at physiological levels in metastatic tumor cells, significantly reduce metastasis without affecting primary tumor size. As such, they provide a window into metastasis-specific signaling. NME1 was identified by its reduced expression in K1735 murine metastatic melanoma sublines as compared to related nonmetastatic sublines [20], and reduced NME1 expression has been associated with aggressive clinical disease (rev. in [21]). Re-expression of NMEs in model systems of breast, hepatocellular, non-small cell lung cancers, melanoma established its metastasis suppressor activity [22–30]. Opposing these solid tumor findings, NME expression in leukemias correlated with advanced disease [31]. NME is a family of genes with the human -H1 and -H2 best studied; in *Drosophila*, the NME homolog *awd* regulates differentiation from imaginal discs and other organs late in development [32, 33]. A unifying functional role for NME/AWD proteins in cellular endocytosis has been established, whereby the signaling of growth factor receptors is modified. In *Drosophila* development, aberrant endocytosis was noted in follicle cells, the trachea, and the nervous system in *awd* null mutants resulting in the deregulation of multiple signaling pathways [34–36]. In both *Drosophila* development and human tumor cell motility and metastasis, an interaction of NME and dynamin has been causal [34, 37, 38]. NME-mediated suppression of tumor cell migration and metastasis has been linked to its interaction with, and promotion of Dynamin 2 (DNM2) oligomerization and function. This interaction facilitated the endocytosis of receptors and other proteins, altering their availability for motility signaling and/or downstream signaling patterns, which in turn affect motility, migration, and metastasis. A dynamin-based mechanism of action has also been reported for the *Drosophila* homolog of NME, AWD, in regulating development and differentiation [34]. NME has been found extracellularly [39], although its packaging and functional consequences in solid tumors are poorly understood (rev. in [40, 41]).

Herein, we defined several parameters of NME in exosomal or liposomal vesicles, asking: (1) Is NME protein secreted into exosomes and does its abundance mirror intracellular levels? (2) Are NME containing exosomes or liposomes taken up by tumor cells and what phenotypes do they confer? (3) For tumor cell secreted exosomes, what other protein cargoes accompany NME? (4) Is NME an active motility, migration and metastasis inhibitory component in extracellular vesicles?

Materials and methods

Cell culture conditions and transfection

Human triple-negative breast cancer cell line MDA-MB-231T (generously provided by Dr. Zach Howard, NCI, Bethesda, MD) and MDA-MB-435 were grown in DMEM (Invitrogen) supplemented with 10% FBS in a humidified 5% CO2 incubator maintained at 37 °C. MDA-MB-231T cells have been authenticated by our laboratory to the ATCC MDA-MB-231 line by short tandem repeat profiling. MDA-MB-435 cells have been attributed to either melanoma or breast carcinoma [42, 43]. MDA-MB-231T (C-Flag) and MDA-MB-435 cells overexpressing NME1 were generated using lentivirus system as described previously [38]. NME1 overexpression profiles of each stable cell line was confirmed by Western blot analysis. Additional methods for cell culture is provided in Supplementary file.

Boyden chamber motility assay

Motility assays were performed as described previously [38, 44]. Briefly, following trypsinization and counting of cells, equal numbers of cells were plated into each upper well of Boyden chamber (0.1 million/ml; 56 µl) in DMEM. Upper and lower chambers were separated by a coated membrane (Polyvinyl membrane 8 µm, coated overnight with 5 µg/ml of collagen type I and washed in PBS for 30'). Cells in the upper wells were allowed to migrate towards chemoattractants placed in the lower wells (1% FBS or conditioned medium, either neat or fractionated- 30 µl, per well) for 4 h in a humidified chamber maintained at 37 °C and 5% CO2. Non-migrated cells were wiped off and cells that had migrated to the undersurface of the membrane were fixed and stained with Diff-Quik solutions (Dade-Behring). All the stained and migrated cells were examined microscopically. Representative areas of each well were counted

to determine the number of cells that had migrated. Mean (± SEM) number of cells migrated are plotted in the graph.

Exosome purification, characterization, and analyses

Exosomes were purified by sequential centrifugation as described previously [6, 11]. Cells were grown in exo-stripped serum containing DMEM for 4 days. Conditioned medium was collected and centrifuged at 500 × g for 10 min to remove any cell contamination and 3000 × g for 20 min at 4 °C to remove any cell debris. Conditioned media was spun at 12,000 g for 20 min at 10 °C to remove any possible apoptotic bodies and large cell debris. Finally, exosomes were collected as a pellet by spinning at 100,000 g for 70 min at 10 °C while its supernatant was used as cytokine fraction. Exosomes were washed in 20 ml PBS and pelleted again by ultracentrifugation (100,000 × g, 70 min, 10 °C) using Type 70 Ti rotor (Beckman Coulter). Exosome size and particle number were analyzed using the LM10 Nanoparticle Tracking Analysis (NanoSight, Malvern Panalytical). For protein quantification, exosome pellets were resuspended in PBS and lysed with 10 × RIPA buffer (Cell Signaling Technology). Protein quantification of the lysed exosomes was performed using the Micro BCA Protein Assay Kit (#23235, ThermoFisher Scientific).

Liposome preparation

Liposomes were prepared using Liposome Kit (L4395, Sigma-Aldrich) containing powdered lipids (Total 90 µmoles/package; Cholesterol, 9 µmol/package, L-α-Phosphatidylcholine (egg yolk), 63 µmol/package, Stearylamine, 18 µmol/package). Powdered lipid was sequentially dissolved in 32 ml PBS, with or without 1000 µg of rNME1, and was incubated for 30 min with rotation at room temperature. The liposomes were put through three freeze–thaw cycles (− 196 °C for 4 min, 42 °C for 4 min) and then extruded 20 cycles through a 100 nm single clean track-etched polycarbonate membrane of NanoSizer MINI STERILE Extruder (TT-002S-010, T&T Scientific). Extruded liposomes were centrifuged (28,000 rpm, 30 min, 4 °C) for separating bound (pellet) and unbound (supernatant) rNME1. Efficiency of rNME1 encapsulation by the liposomes was assessed by Western blot, showing NME1 level at each step of liposome-rNME1 preparation.

Size distribution and zeta potential analysis

Control liposomes and liposomes containing rNME1 were assessed for particle size distributions and zeta potential using ZetaView (Particle Metrix). All samples were diluted in PBS to a final volume of 1 ml and measurement concentrations were found to be 200–300 particles/frame. For every measurement, three cycles were performed by scanning 11 cell positions each at the mobility of 4.38 ± 0.09 µm/sec/V/cm (25 °C). After capture, the videos were analyzed by the ZetaView software.

Experimental metastasis assays

All the animal experiments were performed at NCI-Frederick with an approved National Cancer Institute animal use agreement. Six-week-old Balb/c athymic nude female mice were injected with 7.5×10^5 MDA-MB-231T cells into their lateral tail vein. Exosomes/liposomes were injected three times on 1st, 4th and 7th week post cell inoculation (days 7, 28 and 49). For exosomes, 20 µg exosomes derived from either vector or NME1 overexpressing stable cells in PBS were used per injection along with PBS control. For liposomes, 0.2 mg lipid containing 5 µg rNME1 protein in PBS per injection were used along with control liposomes. Mice were sacrificed 58 days postinjection (for exosomes and 51 days postinjection for liposomes) and the lungs were fixed in Bouin's solution followed by hematoxylin and eosin (H&E) staining. Lung metastatic lesions were counted, and area was measured on H&E step sections using Aperio ImageScope and were reported as a median for each group.

Statistical analyses

All experiments were repeated at least three times unless specified. Statistical significance was calculated by a one-way ANOVA (*, $P < 0.05$; **, $P < 0.01$; ***, $P < 0.001$; ****, $P < 0.0001$). For metastasis Two tailed t-test (nonparametric) was performed comparing median across any two groups, with $P < 0.05$ considered significant (*). ns, nonsignificant.

Results

Extracellular vesicle (EV) fractions from NME1 overexpressing tumor cell lines preferentially inhibit tumor cell motility and migration in vitro

We hypothesized that exosomes from high NME1 expressing tumor cell lines would contain greater NME and be potent inhibitors of tumor cell motility and migration. Two metastatic tumor cell lines were used, MDA-MB-231T and MDA-MB-435, either the naïve cell lines or previously published sets of vector- and NME1 transfectants [38]. Conditioned medium (CM) from each transfectant was used as an attractant for naïve MDA-MB-231T or MDA-MB-435 tumor cell lines in Boyden chamber motility assays. Naïve MDA-MB-231T breast cancer cells, when exposed to the CM of NME1 transfectants, migrated 67% and 53% less than with their respective control

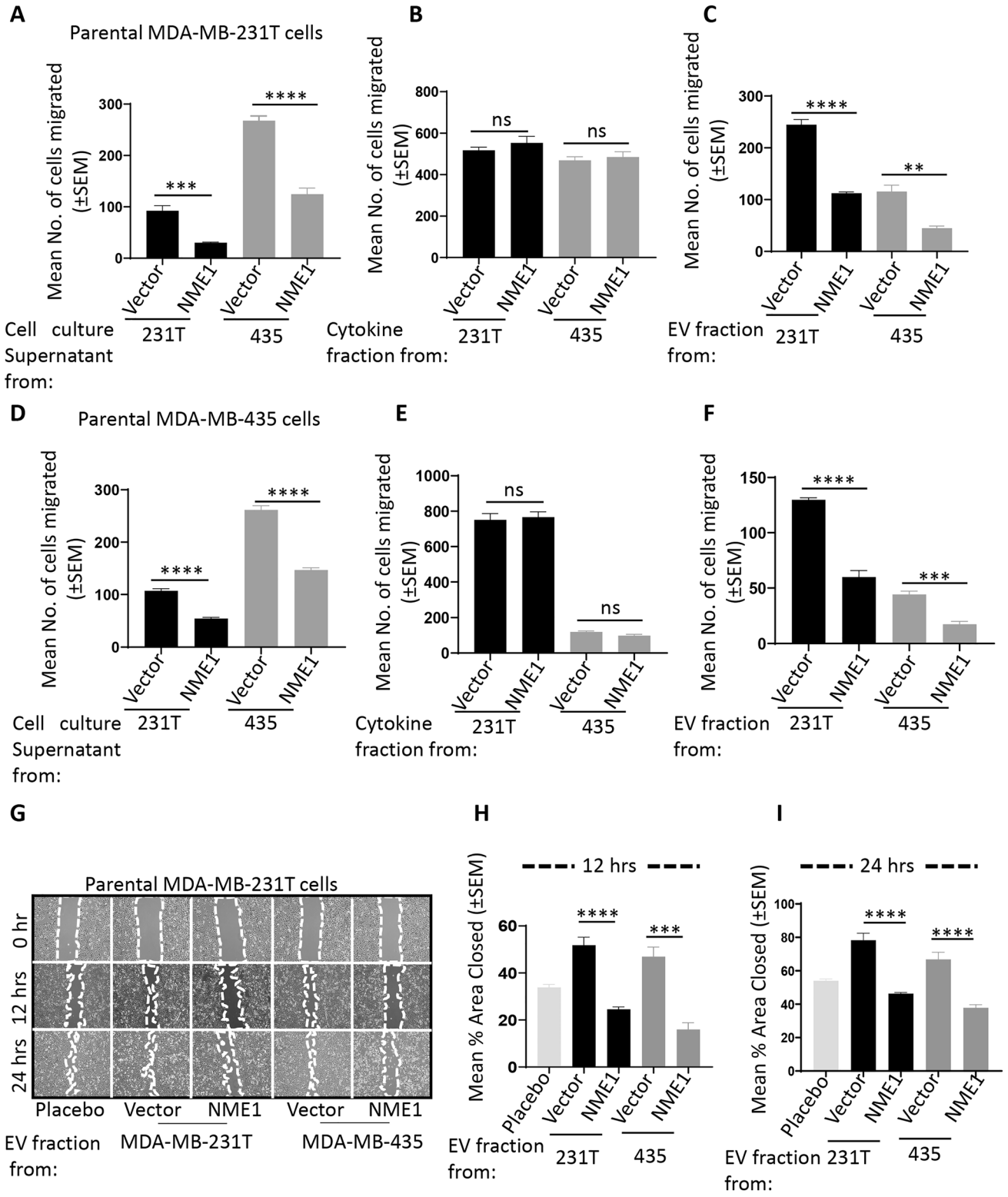

transfectant-derived CMs, respectively (CM of MDA-MB-231T $p = 0.0008$; CM of MDA-MB-435 $p < 0.0001$) (Fig. 1A); similar trends were observed when naïve MDA-MB-435 tumor cells were exposed to the two sets of CM from NME1 and vector transfectants, with migration to CM from NME1 transfectant 48.9% and 43.9% less than that of their respective control transfectant-derived CMs, respectively (both $p < 0.0001$) (Fig. 1D). When the CMs were separated into cytokine and extracellular vesicle (EV) fractions by ultracentrifugation [45], the motility

◂**Fig. 1** NME overexpressing cells conditioned media causes motility suppression (**A–C**), Motility of the MDA-MB-231T metastatic breast cancer cell line was assessed to conditioned medium (CM) collected from vector or NME1 overexpressing stable MDA-MB-231T or MDA-MB-435 cells grown in 10% serum (exo-stripped) containing culture medium for 4 days. CM collected were used as chemoattractant (5% v/v) in Boyden chamber assays to quantify the motility of naïve MDA-MB-231T (**A**). CM from vector or NME1 overexpressing stable MDA-MB-231T or MDA-MB-435 cell line was fractionated into cytokine (**B**) and extracellular vesicle (EV) (**C**) fractions and were used as chemoattractant (neat) for assessing motility of MDA-MB-231T cells. (**D–F**), Similarly, MDA-MB-435 metastatic cancer cell motility was assessed to CM collected from vector or NME1 overexpressing stable MDA-MB-231T or MDA-MB-435 cells. CM was collected and used as chemoattractant (5% v/v) in a Boyden chamber assays to quantify the motility of naïve MDA-MB-435 cells (**C**). CM from vector or NME1 overexpressing stable cells was fractionated into cytokine (**E**) and extracellular vesicles (EV) (**F**) fractions and were used as chemoattractant (neat) for assessing the motility of MDA-MB-435 cells. (**G–I**), Extracellular vesicle (EV) fractions from vector or NME1 transfected MDA-MB-231T or MDA-MB-435 tumor cells (20% v/v) were placed in culture with naïve MDA-MB-231T cells, and their 2D-migration was assessed in scratch assay at 12 (**G–H**) and 24 h (**G–I**). All experiments shown are representative of four replicates and statistical significance was calculated by a one-way ANOVA. ****$P < 0.001$

inhibitory activity of the NME1 transfectant-derived CM resided in the EV fraction (Fig. 1B, C, E, F).

We then asked whether treatment of naïve tumor cells with EV fractions of CM from vector or NME1 transfected cell lines would alter their 2D-migration and motility responses to other attractants. Naïve MDA-MB-231T cells treated directly with the EV fraction from NME1 transfected tumor cell lines migrated less in scratch assays compared to cells exposed to EV from the vector control. The percent of scratch area closed by Vector EV vs NME1 EV was 51.8% vs 24.5% at 12 h, and 78.2% vs 46.3% at 24 h for EVs derived from MDA-MB-231. Similarly, the percent of scratch area closed by vector vs NME1 EV was 46.9% vs 15.9% at 12 h, and 66.7% vs 37.7% at 24 h for EVs derived from MDA-MB-435 cells (Fig. 1G-I). Similar inhibitory results were observed using naïve MDA-MB-435 cells when directly treated with EV fraction of NME1 transfectants compared to its control at both 12 and 24 h (Supplementary Fig. S1A-C). Additionally, each tumor cell line was preincubated for 48 h in the EV fraction of CM, which was then washed off, and tumor cell motility was determined to the combination of growth factors in fetal bovine serum (FBS) using Boyden chamber assays (Supplementary Fig. S1D, E). In each case, naïve tumor cells pretreated with exosomes from NME1 transfected cell lines moved significantly less to FBS compared to those cultured with exosomes from vector transfectants ($p < 0.0001$ for all experiments). The data indicate a broad in vitro tumor motility inhibitory activity of EV fractions of CM from high NME1 expressing tumor cell lines.

Several types of EVs have been described [4, 5, 46]. Nanoparticle tracking analysis of the EV fraction from two sets of NME1 and control transfectants demonstrated characteristics consistent with exosomes with a median size of 121–128 nm from MDA-MB-231T tumor cells and 99 nm from MDA-MB-435 tumor cells (Fig. 2A-B). NME1 overexpressing cell lines produced more exosomes/ml CM than vector controls, a 12.1% increase for MDA-MB-231T tumor cells and a 12.6% increase for MDA-MB-435 tumor cells. Transmission Electron Microscopy (TEM) confirmed a typical exosome structure and varying size of approximately 50–150 nm (Supplementary Fig. S2A, B).

Exosomes from high NME1-expressing tumor cell lines contain greater NME1

We determined NME1 levels in cellular and exosomal lysates from two sets of control and NME1 transfectants. NME1 levels were elevated in exosomes from the NME1 transfectants (Fig. 2C-D). As a control for exosome isolation, exosome lysates were enriched in TSG101, a component of the endosomal sorting complex required for transport (ESCRT) [47], Alix, an ESCRT-associated protein involved in exosome budding [4], Rab 27A, involved in exosome release [4], and Flotillin 1, which modulates exosome biogenesis and cargo [48].

A similar analysis of cellular and exosome lysates of multiple breast cell lines is shown on Fig. 2E-F. The immortal breast cell line MCF-10A exhibited high cellular NME1 levels but virtually no exosome expression of either NME1, RAB27A or ALIX. Six tumorigenic, low-nonmetastatic breast cancer lines exhibited relatively high cellular NME1 levels, with five of the six having exosomes containing NME1; ALIX and RAB27A levels tended to covary with NME1 in exosomes. Cellular NME1 levels of three metastatic breast cancer cell lines were lower than that of non-metastatic lines, but NME1 was appreciably lower in their exosomes and covaried with ALIX. RAB27A was low in two metastatic cell lines and moderate in the remaining two metastatic cell lines. The lack of NME1 in exosomes from an immortal breast cell line suggests that exosome sorting mechanisms may vary between normal and tumor cells, if the findings replicate in additional cell lines. NME1 incorporation into exosomes was near universal in tumor cell lines and showed a general concordance with cellular levels.

The NME1 content of exosomes from tumor cell lines appeared to rely on both cellular NME1 expression level and the presence of exosome generating machinery (Fig. 2E-F). We then asked if the combination of high tumor NME1 and high exosome biogenesis activity had prognostic significance in breast cancer (Fig. 2G and Supplementary Fig. S3A-B). Using the TCGA breast cancer database progression free survival (PFS) was plotted by primary tumor

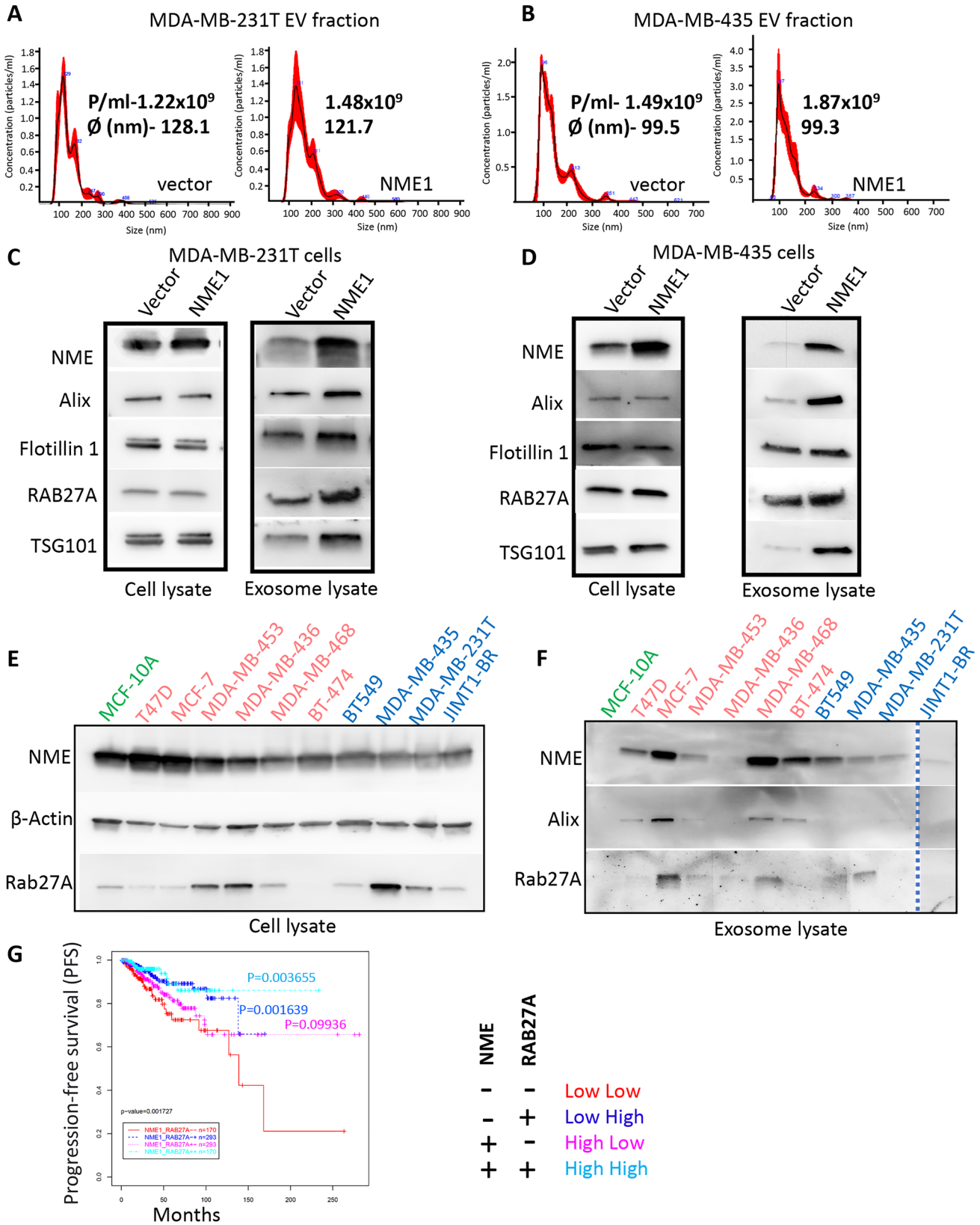
A
MDA-MB-231T EV fraction
P/ml-1.22x10⁹
Ø (nm)- 128.1
vector
1.48x10⁹
121.7
NME1
Concentration (particles/ml)
Size (nm)
B
MDA-MB-435 EV fraction
P/ml- 1.49x10⁹
Ø (nm)- 99.5
vector
1.87x10⁹
99.3
NME1
C
MDA-MB-231T cells
Vector
NME1
NME
Alix
Flotillin 1
RAB27A
TSG101
Cell lysate
Exosome lysate
D
MDA-MB-435 cells
E
MCF-10A
T47D
MCF-7
MDA-MB-453
MDA-MB-436
MDA-MB-468
BT-474
BT549
MDA-MB-435
MDA-MB-231T
JIMT1-BR
β-Actin
Rab27A
F
G
Progression-free survival (PFS)
P=0.003655
P=0.001639
P=0.09936
p-value=0.001727
Months
NME
RAB27A
Low Low
Low High
High Low
High High

◂**Fig. 2** Extracellular vesicles from metastatic cell lines have characteristics of exosomes (**A**–**B**), Extracellular vesicle (EV) fractions isolated from the conditioned medium of vector- and NME1 overexpressing MDA-MB-231T (**A**) and MDA-MB-435 (**B**) cells were assessed for particle size distribution analysis and number/ml using NanoSight. (**C**–**D**), Western blotting analysis of total cell lysates and CM-derived EV fractions from MDA-MB-231T (**C**) and MDA-MB-435 (**D**) cells. (**E**–**F**), Western blot analysis of exosomes and total cell lysates of various breast cancer cell lines with varying metastatic status: nontumorigenic, green; tumorigenic, poorly or nonmetastatic, pink; metastatic, blue. (**G**), Progression free survival (PFS) of breast cancer patients (TCGA dataset) was plotted using KM-plot for two genes NME1 and RAB27A. High expression of both NME1 and Rab27A resulted in the best PFS and, conversely, low expression of both genes resulted in the poorest PFS, with mixed gene expression combinations in between

median expression of NME1 and/or Rab27A expression, the latter a marker of exocytotic pathways [49] (Fig. 2G, Supplementary Fig. S3A-B). High expression of both NME1 and Rab27A resulted in the best PFS and, conversely, low expression of both genes resulted in the poorest PFS, with mixed gene expression combinations in between. Rab27A itself was prognostic while NME1 expression showed a trend.

Exosomes enter recipient tumor cell lines and alter NME1 expression

If NME1-containing exosomes were to affect metastasis-associated functions, they must fuse with tumor cells and deploy their contents at sufficient levels. Exosomes from the CM of two sets of control- and NME1 transfectants were labelled using the ExoGlow-membrane EV labelling kit. Labelled exosomes were added to target cell cultures (15% v/v) and their cellular uptake was visualized using fluorescent microscopy 24 h post-treatment. Red fluorescently labelled exosomes derived from vector or NME1 overexpressing MDA-MB-435 or MDA-MB-231 stable cells were observed in naïve MDA-MB-23T and MDA-MB-435 cancer cells (Fig. 3A-B and Supplementary Fig. S4 A-B). There was no observable difference in red fluorescence between cells treated with exosomes from vector or NME1 transfectants, suggesting no difference in uptake efficiency. Naïve cancer cells treated with exosomes derived from NME1 overexpressing MDA-MB-435 or MDA-MB-231T cells showed an increase in NME1 expression on western blots compared to vector exosome treated cells (Fig. 3C-D). These data argue that exosomal NME is taken up by tumor cells and results in discernable increases in cellular levels.

Analysis of the exosome proteome

Exosomes are known to contain thousands of proteins and nucleic acids [46]. We asked if NME1 was the only differentially expressed protein in exosomes from control- and NME1 transfected tumor cell lines. A mass spectroscopy analysis of vector and NME1 transfected MDA-MB-435 tumor cell exosomes identified over 600 proteins (Supplementary Table S1 and S2) of which 392 were differentially expressed by ≥ 1.5-fold (Fig. 4A-B). The most abundant exosomal protein identified was NME1 (red arrow). Its degree of overexpression could not be quantified as it was not detected in the vector transfectant exosomes. Exosome-associated proteins were identified and provide support for the specificity of the input (Supplementary Fig. S5A-B). Included among the differentially expressed proteins were additional metastasis-associated proteins including RAC1, RHOA and TSP1. In agreement, an IPA pathway analysis of the differentially expressed exosomal proteins identified metastasis-associated pathways including integrin signaling, epithelial adherens junction, actin cytoskeleton, RhoGDI, paxillin, RHO and RAC signaling that could, in themselves, influence metastasis (Fig. 4C). Endocytic pathways, known to be a target of NME1 action, were also identified by IPA pathway analysis including clatherin-mediated endocytosis signaling, virus entry via endocytic pathways, and caveolar-mediated endocytosis signaling (Fig. 4C).

NME-containing exosomes show only a trend in reducing metastatic outgrowth

We hypothesized that exosomes from NME1 overexpressing cell lines would be metastasis suppressive. Exosomes from vector and NME1 overexpressing MDA-MB-435 tumor cells were collected and stored at − 80 °C. Figure 5A demonstrates that the exosomes from the NME1 transfected line contained greater NME1 protein than those from the corresponding vector transfectant. An experimental metastasis assay was performed in which MDA-MB-231T tumor cells were injected into the tail veins of nude mice on day 0. Reasoning that exosomes may not produce a permanent change in phenotype, three exosome injections were spread out over the 9-week experiment (20 µg protein in PBS/injection, or PBS) (Fig. 5B). Representative formalin-fixed, paraffin embedded (FFPE) sections of lungs at the experimental endpoint showed multiple metastases that declined in the NME1 exosome treated arm (Fig. 5C). PBS treated mice developed a median of 23.5 metastases per lung section. Injection of exosomes from the vector transfectant resulted in 80 metastases per section, an augmentation of metastasis consistent with prior literature [5, 46]. Injection of exosomes from the NME1 overexpressing cell line resulted in a median of 31 metastases per section, a 61.25% reduction from the vector control, although only a statistical trend ($p = 0.10$) (Fig. 5D). Analysis of metastasis size revealed similar trends. The median size of metastases from mice treated with PBS, exosomes from vector transfectant and

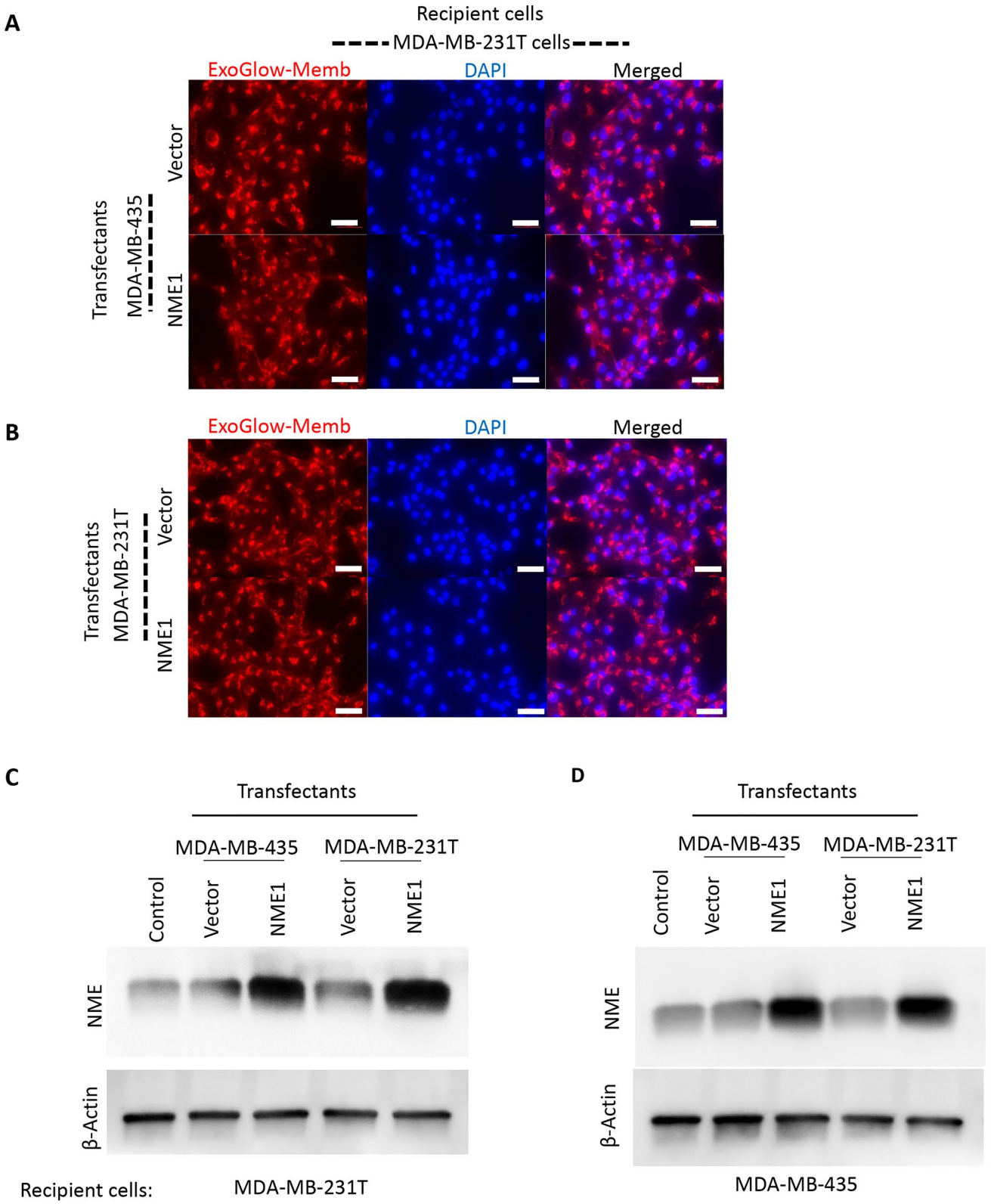
A
Recipient cells
MDA-MB-231T cells
ExoGlow-Memb
DAPI
Merged
Transfectants
MDA-MB-435
Vector
NME1
B
ExoGlow-Memb
DAPI
Merged
Transfectants
MDA-MB-231T
Vector
NME1
C
Transfectants
MDA-MB-435
MDA-MB-231T
Control
Vector
NME1
Vector
NME1
NME
β-Actin
Recipient cells:
MDA-MB-231T
D
Transfectants
MDA-MB-435
MDA-MB-231T
Control
Vector
NME1
Vector
NME1
NME
β-Actin
MDA-MB-435

◂**Fig. 3** Exosomes enter recipient tumor cell lines and alter total NME1 expression (**A**–**B**), Naïve MDA-MB-231T cells were incubated with (15% v/v) membrane labelled exosomes from vector- or NME1 overexpressing MDA-MB-435 (**A**) and MDA-MB-231T cells (**B**) and their cellular uptake was visualized using fluorescent microscopy 24 h post-treatment. Representative images are shown at ×40 magnification. Scale bar, 50 µm. (**C**), Naïve MDA-MB-231T cells were treated with exosomes derived from vector- or NME1 overexpressing MDA-MB-435 or MDA-MB-231T cells and total cellular NME1 expression was assessed by western blots. (**D**), Naïve MDA-MB-435 cells were treated with exosomes derived from vector- or NME1 overexpressing MDA-MB-435 or MDA-MB-231T cells and NME1 expression was assessed by western blots

NME1 transfectant were 4,185,752 μm^2, 13,865,596.5 μm^2 and 7,527,619 μm^2, respectively ($p = 0.24$) (Fig. 5E).

Liposomes containing rNME1 recapitulate tumor motility and migration suppressor functions

The lack of significant metastasis inhibition by exosomes from NME1 overexpressing tumor cells, despite robust motility and migration inhibition, may have several causes: (1) Other components of the exosomes may exert pro-metastatic influences, (2) sufficient NME may not have been delivered in vivo, or (3) extracellular vesicular NME may be motility but not metastasis regulatory. To answer at least some of these questions we turned to a larger vesicle capable of delivering increased cargo loads of a single protein. Liposomes are one of several nanomaterial platforms to deliver drugs or proteins, and offer the potential advantages of higher capacity, biocompatibility, and easy loading [50].

A liposomal vector was developed to deliver NME1 in vitro and in vivo. A cholesterol, L-α-phosphatidylcholine and stearylamine based liposome was used as a protein carrier and loaded with partially purified recombinant bacterial NME1 (rNME1) (Supplementary Figs. S6A and S6B). Loading efficiency was estimated at > 90% by western blot as compared to total protein input (Supplementary Fig. S6C). The control- and NME1 loaded liposomes were cationic in nature and had comparable diameters (220.9 and 198.6 nm) as measured by Zeta View NTA (Fig. 6A, B) and Transmission Electron Microscopy (TEM) (Fig. 6C, D).

To assess the delivery of rNME1 to target cells using liposomes, naïve MDA-MB-231T or MDA-MB-435 cells were treated with either control liposomes or liposomes containing a labelled rNME1 and its delivery was confirmed by western blot (Fig. 6E, F).In Boyden chamber motility assays, the control liposome preparation was 25% and 22% motility inhibitory to the MDA-MB-231T and MDA-MB-435 tumor cell lines, respectively. This compares to 76% and 72% motility inhibition of the same lines by rNME1 containing liposomes (both $p < 0.0001$) (Fig. 6 G–H). The migration of naïve MDA-MB-231T and MDA-MB-435 tumor cells after incubation with rNME1 containing liposomes was reduced by 22% and 29%, respectively (both $p < 0.0001$) (Fig. 6 I-J and Supplementary Fig. S6D-E). The data indicate that a rNME1 liposomal preparation recapitulated motility and migration suppressive phenotypes of tumor cell derived exosome containing NME1.

Liposomes containing rNME1 are metastasis suppressive

In an initial toxicity dose response analysis using liposomes loaded with rNME1 protein, a dose of 0.2 mg lipid containing 5 µg rNME1/mouse was found to be safe (Supplementary Fig. S7A and B). A similar experimental metastasis design was used for liposome injections as was used for exosomes (Fig. 7A). MDA-MB-231T breast cancer cells were injected into the tail veins of nude mice, and liposome injections spread out over the 7-week experiment (1st, 4th and 7th week). Representative photographs of lung sections from the two groups are shown on Fig. 7B. Median lung metastases per histologic section was 158 using control liposomes and 15 in the rNME1 liposome group, 90.5% lower than the control liposome group ($P = 0.016$) (Fig. 7C). A similar reduction in metastasis size was observed, from a median of 4.49×10^7 μm^2 using control liposomes to 3.63×10^6 μm^2 in the rNME1 group ($P = 0.020$) (Fig. 7D).

Lung sections from all three groups were stained by immunohistochemistry and presented with H&E and rabbit IgG isotype control (Fig. 7E). NME1 protein was cytoplasmic in nests of tumor cells and was darker in intensity in those animals treated with rNME1-containing liposomes, confirming uptake in vivo. Increased NME1 expression was also observed in uninvolved lung, suggesting that liposomes also fused with normal cells (Fig. 7E). No specific staining was observed with rabbit IgG isotype control.

Liposomal and exosomal NME modulates the endocytic process

Since the endocytic process has been found to be integral to NME phenotypes in both tumor metastasis and *Drosophila* development, we asked if exosomal or liposomal NME1 delivery followed the same pathway. We previously reported

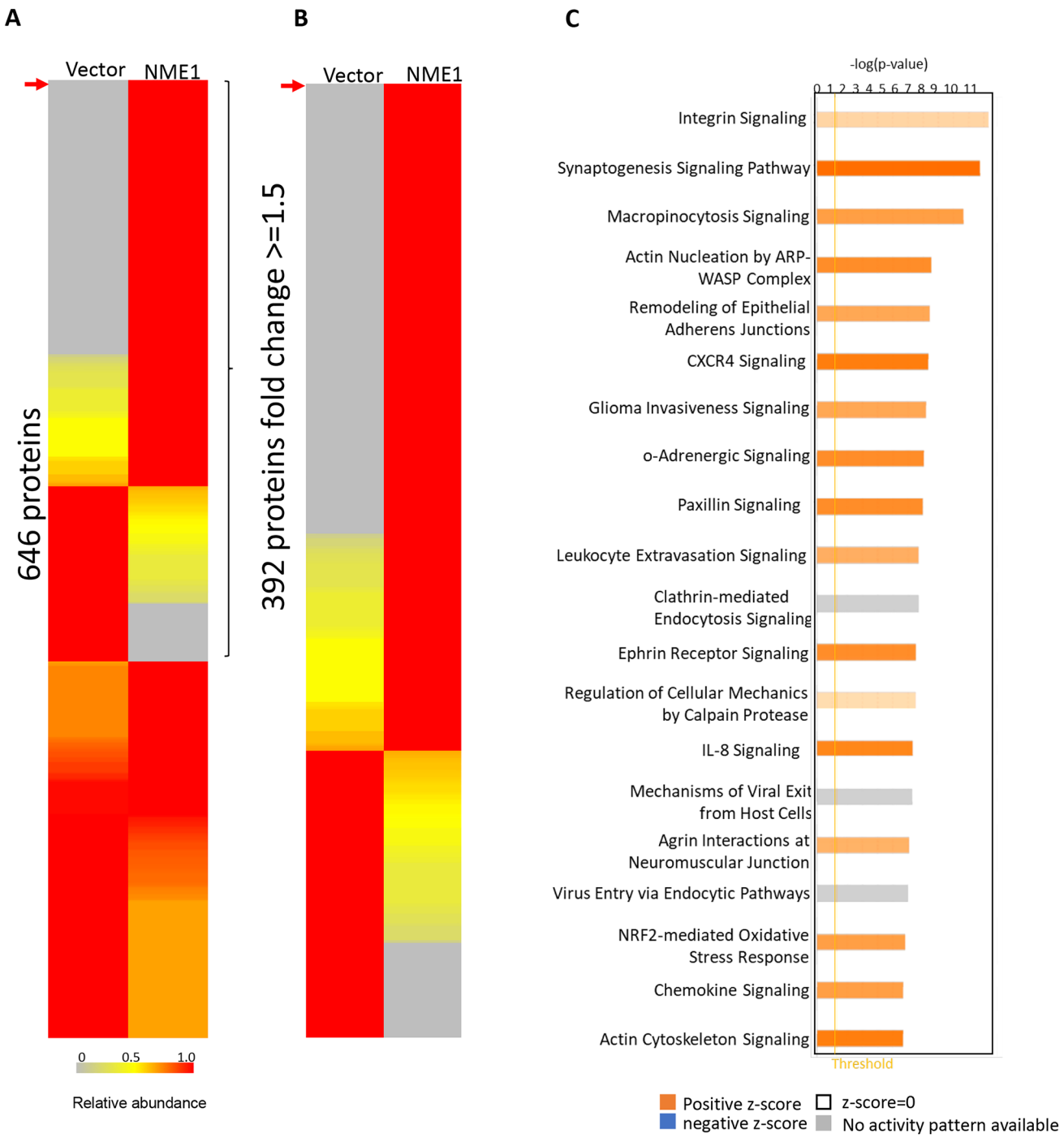

Fig. 4 NME1 is a major component of the exosome proteome (**A**), Mass spectroscopy analysis of vector- and NME1 transfected MDA-MB-435 tumor cell derived exosomes was performed and a heat map depicting the relative abundance of 646 proteins identified across the two samples is shown. (**B**), Heat map depicting the relative abundance of 392 proteins differentially expressed (≥ 1.5-fold change) between exosomes of vector- and NME1 overexpressing cells are plotted. The color key indicates the relative abundance of each protein (0 to 1.0) across the two samples. The most abundant exosomal protein identified was NME1 (red arrow). (**C**), IPA pathway analysis of the differentially expressed exosomal proteins highlights involvement of several pathways

that NME1 overexpressing breast cancer cell lines showed increased endocytosis of transferrin receptor and EGF receptor (EGFR) due to a NME1-Dynamin2 interaction regulating endocytic vesicle scission leading to motility and metastasis suppression [38]. In vitro, naïve MDA-MB-231T and MDA-MB-435 tumor cell lines demonstrated increased endocytosis of EGFR when incubated with exosomes derived from NME1 overexpressing cells (Fig. 8A–B and Supplementary Fig. S8A-B) or liposomes containing rNME1 (Fig. 8C–D and Supplementary Fig. S8C-D), confirming that exosomal NME1 initiates known intracellular mechanisms of action.

To determine if EGFR trafficking and activity was altered in vivo, lung sections from the liposome experiment were stained by immunohistochemistry for total and phospho-EGFR (Fig. 8E and Supplementary Fig. S9A-B). Total EGFR was both cytoplasmic and membranous in tumor cell nests, and of variable intensity in the experimental arms. For mice treated with rNME1-containing liposomes, lung sections expressed less EGFR staining with a heterogenous staining pattern. To examine EGFR activation, an antibody to pEGFR (1068 + 1092) demonstrated prominent staining in lung sections from the control liposome arm but markedly lower staining in the lung sections from animals treated with rNME1-containing liposomes, consistent with previous data that NME1-increased endocytosis resulted in EGFR inactivation. No specific staining was observed with rabbit IgG isotype control (Supplementary Fig. S9A).

Discussion

Our data support a role for NME1 protein in extracellular vesicles in the regulation of tumor cell motility, migration and metastasis, a finding that is potentially translatable. We show that many breast cancer cell lines secrete exosomes containing NME1 in rough proportion to their intracellular levels, as opposed to a single nontumorigenic breast cell line. Exosomes from two NME1-transfected cell lines, or synthetic liposomes loaded with partially purified rNME1, released their contents into naïve tumor cells, altering EGFR endocytic functions, and inhibiting tumor cell motility and migration in vitro. Only liposomes, containing greater NME and devoid of other cell-derived proteins found in exosomes, inhibited experimental metastasis at levels comparable to NME1 transfection.

The metastasis suppressors stand as optimal candidates for vesicle-based therapeutic approaches. The metastasis suppressor KAI1 has also been shown to be exported into exosomes in colorectal cancer [51]. An extracellular role for the NME family of proteins (NME1-8) has been previously proposed in stem cells, leukemias and solid tumors, but issues exist, including whether findings are due to soluble or vesicular protein, the receptor if a soluble protein, the participation of other proteins if an exosome, and phenotypic consequences. NME proteins lack a signal peptide for secretion. For leukemias NME proteins are found in the bloodstream, have prognostic ability [31], and recombinant NME proteins stimulated tumor proliferation [52]; a receptor has not been identified. In solid cancer models soluble NME has been detected [53, 54] as well as NME in extracellular vesicles [55, 56]. Data presented herein confirm the incorporation of NME1 into exosomes in breast cancer cell lines, and identify their functional consequences in vitro on naïve tumor cells.

Exosomes from a high NME1 expressing cell line showed only a trend in reduced metastasis numbers and size in vivo. Additional testing of other doses and schedules was limited by the exorbitant tissue culture requirements for exosome collection. NME1 encapsulated in liposomes significantly reduced experimental metastasis to levels lower than either the PBS or control liposome injected arms, with a corresponding diminution in lesion size. The data suggest the hypothesis that liposomal or similar delivery of NME protein may have a metastasis preventive effect. To date, no signs of toxicity have been observed. To our surprise empty liposomes increased experimental metastasis. It is possible that the lipid composition of liposomes is critical to baseline effects on metastasis, as lipids in a variety of forms cause increased metastasis [57–59]. Many other variables will be tested in future experiments including liposome structure, dose and schedule of inoculation, and a metastasis shrinking versus preventive effect. NME may be particularly suitable for this type of delivery as it is a very long-lived protein. Liposomes have been widely tested preclinically to deliver drugs and biologicals and several clinical trials are being conducted [60] (https://clinicaltrials.gov/ct2/results?cond=cancer&term=liposome+or+liposomal&cntry=&state=&city=&dist=).

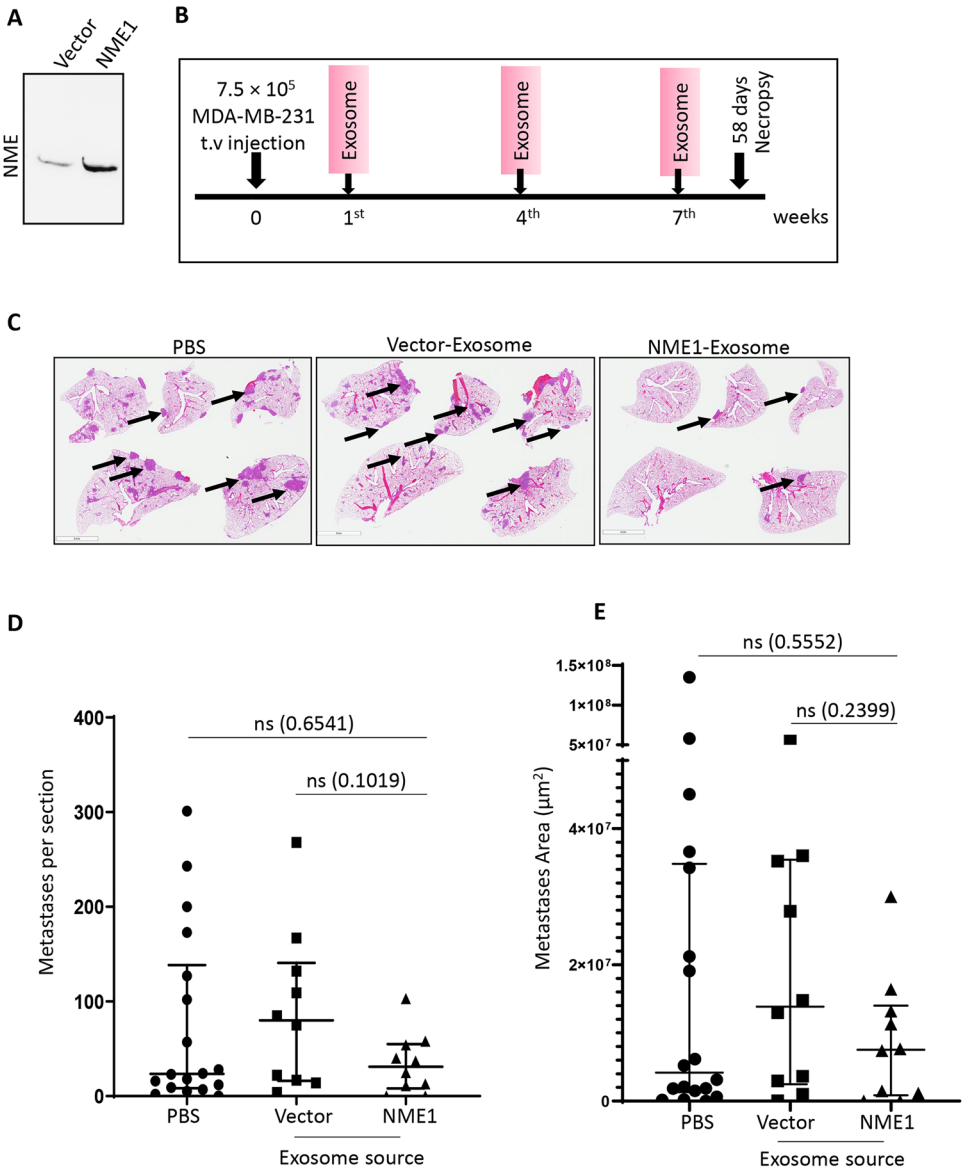

Fig. 5 Exosomes from NME1 overexpressing cells showed a trend of decreased metastasis (**A**), Western blot analysis of exosomes collected from vector- and NME1 overexpressing MDA-MB-435 tumor cells and used for in vivo experiments. (**B**), Diagrammatic representation of experimental metastasis assay in which MDA-MB-231T tumor cells were injected into the tail veins of nude mice on day 0. Exosomes were injected three times on 1st, 4th and 7th week (20 µg protein in PBS/injection, or PBS) over the 9-week experiment. (**C**), Lungs from mice 58 d postinjection. The lungs were fixed in Bouin's solution, sectioned, and stained hematoxylin and eosin. A representative image of each group is presented, with arrows pointing to several metastases. (**D**), Total number of lung metastases per histologic section through the center of the lungs from each mouse. (**E**), Total area of all metastases in the lung section described above. Data are presented as scatter plot showing median with interquartile range. Each dot represents a single mouse. Two tailed t-test (nonparametric) was performed comparing median across any two groups, with $P < 0.05$ considered significant (*). ns, nonsignificant

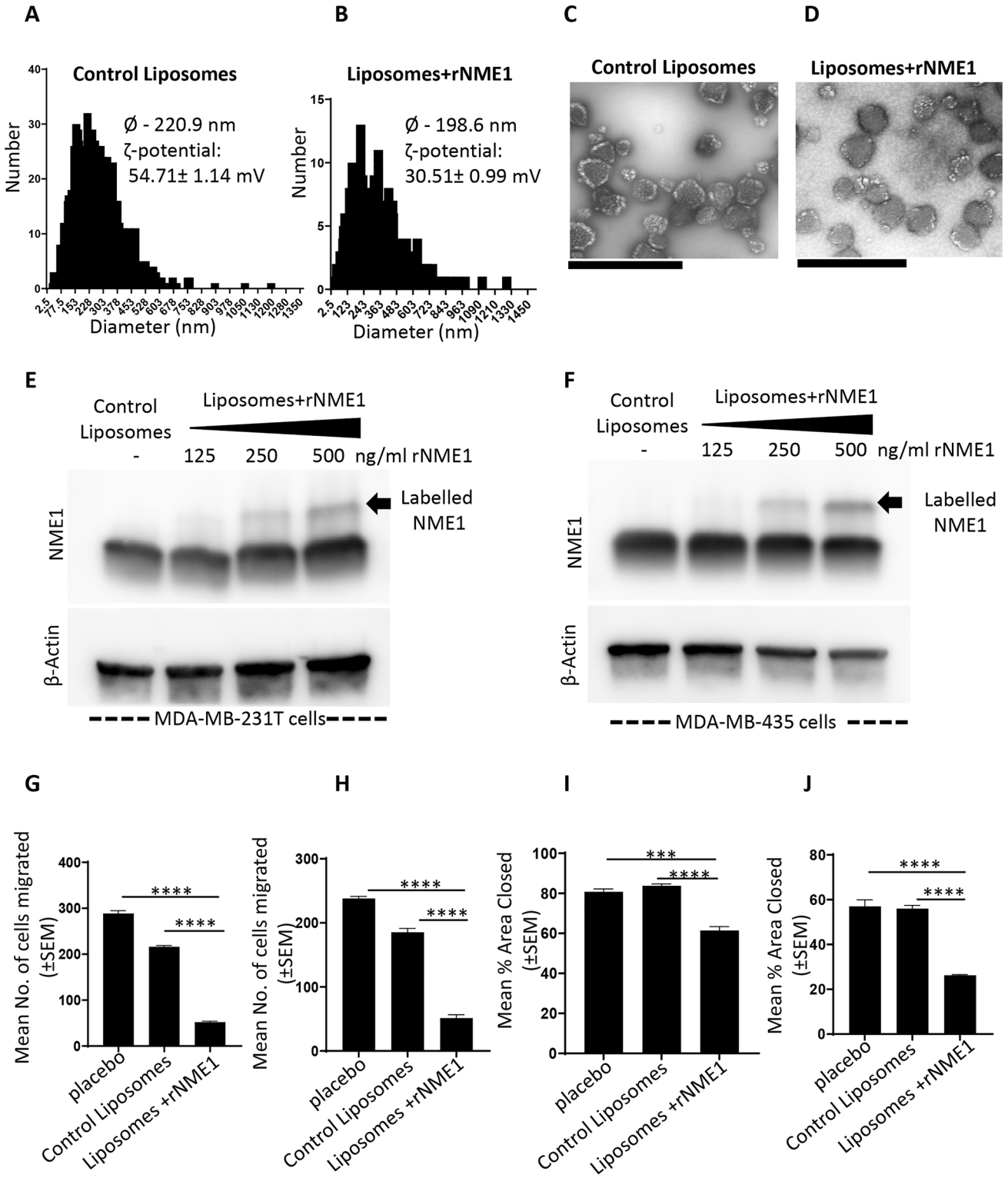

Fig. 6 Liposomes containing rNME1 suppress tumor cell motility and migration (**A**–**B**), Control (empty) liposomes and liposomes containing partially purified recombinant rNME1 were assessed for particle size distributions and zeta potential using ZetaView (Particle Metrix). (**C**–**D**), Representative Transmission electron microscopy images of control liposomes and liposomes containing rNME1. Scale bar: 600 nm. (**E**–**F**), Western blot of naive MDA-MB-231T and MDA-MB-435 cells treated with increasing doses of liposomes containing rNME1 or control liposomes. The mobility of the labelled NME1 is shown (arrow). (**G**-**J**), Naïve MDA-MB-231T (**G**) and MDA-MB-435 (**H**) cells were treated with control liposomes and liposomes containing rNME1 (250 ng/ml) for 24 h. Following this, Boyden chamber motility assays were performed on the treated cells using 1% serum as chemoattractant. The treated cells were also assessed for 2D migration assay (**I** and **J**, respectively) and % area closed was plotted

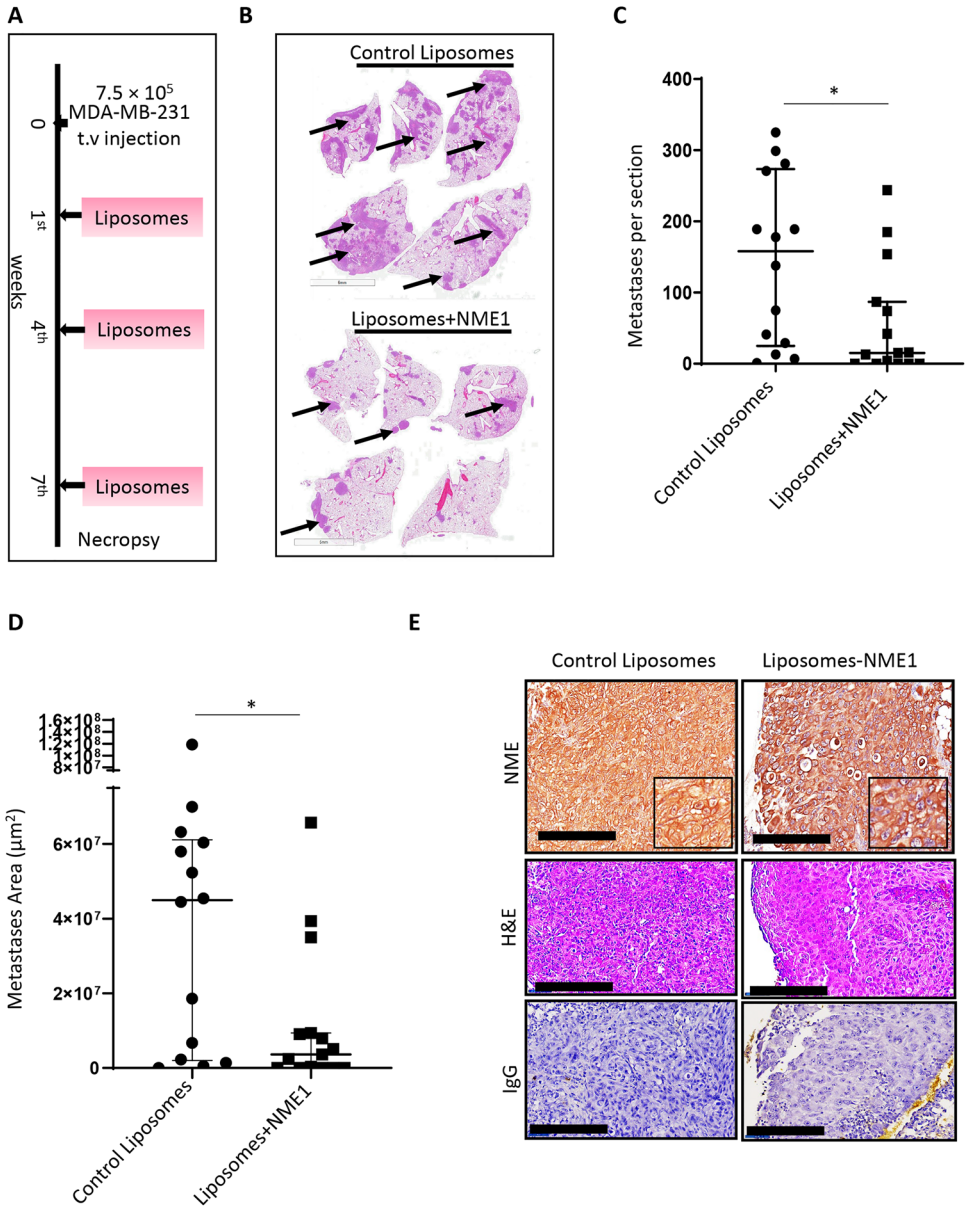

Fig. 7 Liposomes containing rNME1 are metastasis suppressive (**A**), Diagrammatic representation of experimental metastasis assay in which MDA-MB-231T tumor cells were injected into the tail veins of nude mice on day 0. Three experimental arms compared control liposomes alone, liposomes containing 5 µg rNME1 protein in PBS or PBS without any liposomes. Liposome preps were injected three times on 1st, 4th and 7th week postinjection (0.2 mg control lipid alone or lipid containing-5 µg rNME1 /injection) over the 8-week experiment. (**B**), At 51 days postinjection, the mice were necropsied, and the lungs were fixed in Bouin's solution followed by sectioning and hematoxylin and eosin staining. A representative image of each group is presented (arrows pointing to several metastases). (**C**), All metastases in a section through the middle of each mouse lung were counted. (**D**), The area of all metastases in lung section described above was determined, and the median and interquartile ranges plotted. Each dot represents a single mouse. Two tailed t-test (nonparametric) was performed comparing median across any two groups, with $P < 0.05$ considered significant (*). ns, nonsignificant. (**E**), Immunohistochemical staining was conducted on sections of lungs from five mice per experimental arm for NME1 protein. Representative images showing lung metastases with magnified inserts. Scale bar: 200 µm

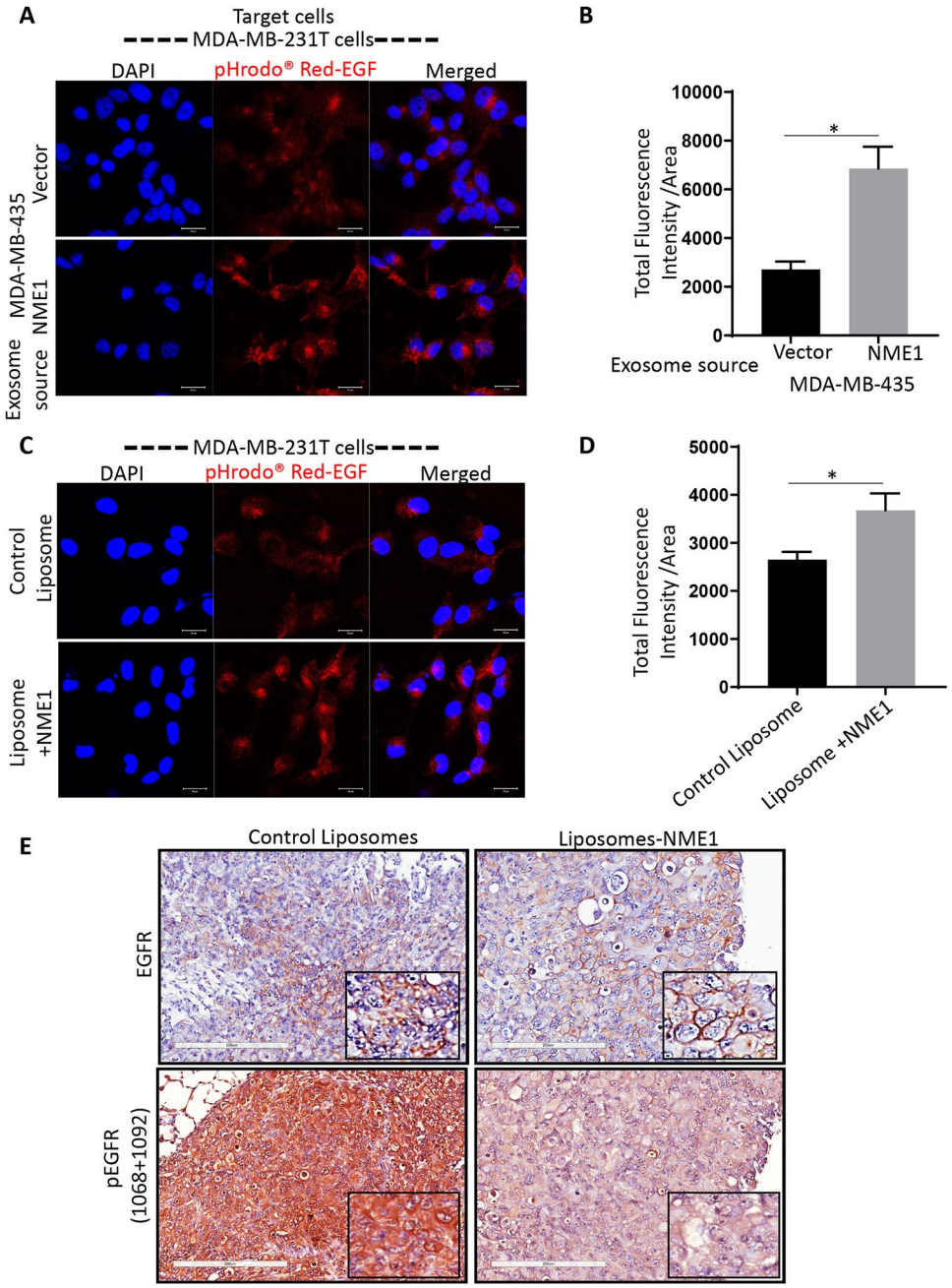

Fig. 8 Exosomal or liposomal NME1 alter EGFR activity in vitro (**A**–**B**), Naïve MDA-MB-231T (**A**) cells were incubated with exosomes (5% v/v) derived from vector- and NME1 overexpressing MDA-MB-435 cells for 24 h. Post treatment, cells were incubated at 4 °C for 10 min, washed with cold PBS and then incubated with pHrodo Red-EGF for 15 min at 37 °C. pHrodo Red-EGF will only fluoresce when in an acidic environment of intracellular vesicles. Cells were fixed in PFA and nuclei stained with DAPI (blue). (**A**), Representative images are shown at × 63 magnification. Scale bar, 20 µm. (**B**), Quantification of pHrodo Red-EGF endocytosis in the MDA-MB-231T target cells was performed using Zeiss software (ZEN). (**C**–**D**), Naïve MDA-MB-231T cells were incubated with control liposomes or liposomes containing rNME1 (~ 250 ng rNME1/ml) for 24 h. Post treatment cells were assessed for pHrodo Red-EGF uptake as described above (**C**). (**D**), Quantification of pHrodo Red-EGF endocytosis in the MDA-MB-231T target cells. (**E**), Immunohistochemical staining was conducted on sections of lungs from five mice per experimental arm for total EGFR and pEGFR (1068 and 1092). Representative images are shown with magnified inserts. Scale bar: 200 µm. All experiments shown are representative of three replicates (at least) and statistical significance was calculated by two tailed t-test. *$P < 0.05$

Supplementary Information The online version contains supplementary material available at https://doi.org/10.1007/s10585-022-10182-7.

Acknowledgements The authors thank the NCI confocal and FACS facilities. Electron Microscopy was performed at the NICHD Microscopy & Imaging Core with the assistance of Chip Dye. P. Steeg is supported by the Intramural Program of the NCI, NIH [Investigator-Initiated Intramural Research Projects (ZIA). Project #1ZIASC000892-33, Application #9344091]. This work is supported by an NIH intramural grant.

Author contributions Conception and design: IK, PSS; Development of methodology: IK, PSS; Acquisition of data (provided animals, provided facilities, etc.): IK, BG, AH, SD, DCL; Analysis and interpretation of data (e.g., statistical analysis, biostatistics, computational analysis): IK, HHY, MPL, BG, DCL, PSS; Writing, review, and/or revision of the manuscript: IK, PSS, DCL; Administrative, technical, or material support (i.e., reporting or organizing data, constructing databases): IK; Study supervision: IK, DCL, PSS.

Funding This work is supported by a National Institutes of Health (NIH) intramural grant.

Data availability All data generated or analyzed during this study are included in this published article [and its supplementary information files].

Declarations

Competing interests The authors declare no competing interests.

Conflicts of interest No potential conflicts of interest were disclosed.

References

1. Steeg PS (2016) Targeting metastasis. Nat Rev Cancer 16(4):201–218
2. Dvorak HF et al (1981) Tumor shedding and coagulation. Science 212(4497):923–924
3. Crawford N (1971) The presence of contractile proteins in platelet microparticles isolated from human and animal platelet-free plasma. Br J Haematol 21(1):53–69
4. Mashouri L et al (2019) Exosomes: composition, biogenesis, and mechanisms in cancer metastasis and drug resistance. Mol Cancer. https://doi.org/10.1186/s12943-019-0991-5
5. Zhang L (1871) Yu DH (2019) Exosomes in cancer development, metastasis, and immunity. Biochimica Et Biophysica Acta-Rev Cancer 2:455–468
6. Peinado H et al (2012) Melanoma exosomes educate bone marrow progenitor cells toward a pro-metastatic phenotype through MET. Nat Med 18(6):883–891
7. Rodrigues G et al (2019) Tumour exosomal CEMIP protein promotes cancer cell colonization in brain metastasis. Nat Cell Biol 21(11):1403–1412
8. Costa-Silva B et al (2015) Pancreatic cancer exosomes initiate pre-metastatic niche formation in the liver. Nat Cell Biol 17(6):816–826
9. Ono M et al (2014) Exosomes from bone marrow mesenchymal stem cells contain a microRNA that promotes dormancy in metastatic breast cancer cells. Sci Signal. https://doi.org/10.1126/scisignal.2005231
10. Zhang HY et al (2017) Exosome-delivered EGFR regulates liver microenvironment to promote gastric cancer liver metastasis. Nat Commun. https://doi.org/10.1038/ncomms15016
11. Hoshino A et al (2015) Tumour exosome integrins determine organotropic metastasis. Nature 527(7578):329–335
12. Ichikawa H et al (2021) Exosome transfer between pancreatic-cancer cells is associated with metastasis in a nude-mouse model. Anticancer Res 41(6):2829–2834
13. Wang D et al (2020) Exosome-encapsulated miRNAs contribute to CXCL12/CXCR4-induced liver metastasis of colorectal cancer by enhancing M2 polarization of macrophages. Cancer Lett 474:36–52
14. Wang KY et al (2020) An exosome-like programmable-bioactivating paclitaxel prodrug nanoplatform for enhanced breast cancer metastasis inhibition. Biomaterial. https://doi.org/10.1016/j.biomaterials.2020.120224
15. Corrado C et al (2013) Exosomes as intercellular signaling organelles involved in health and disease: basic science and clinical applications. Int J Mol Sci 14(3):5338–5366
16. Shimbo K et al (2014) Exosome-formed synthetic microRNA-143 is transferred to osteosarcoma cells and inhibits their migration. Biochem Biophys Res Commun 445(2):381–387
17. Mao G, Mu Z, Wu D (2021) Exosome-derived miR-2682–5p suppresses cell viability and migration by HDAC1-silence-mediated upregulation of ADH1A in non-small cell lung cancer. Hum Exp Toxicol 40(12 suppl):S318–S330. https://doi.org/10.1177/09603271211041997
18. Shang D, Liu Y, Chen Z (2022) Exosome-transmitted miR-128 targets CCL18 to inhibit the proliferation and metastasis of urothelial carcinoma. Frontiers Mol Biosci. https://doi.org/10.3389/fmolb.2021.760748
19. Feng CX et al (2021) Folic acid-modified Exosome-PH20 enhances the efficiency of therapy via modulation of the tumor microenvironment and directly inhibits tumor cell metastasis. Bioactive Mater 6(4):963–974
20. Steeg PS et al (1988) Evidence for a novel gene associated with low tumor metastatic potential. J Nat'l Cancer Inst 80:200–204
21. Hartsough MT, Steeg PS (2000) Nm23/nucleoside diphosphate kinase in human cancers. J Bioenerg Biomembr 32(3):301–308
22. Leone A et al (1991) Reduced tumor incidence, metastatic potential, and cytokine responsiveness of nm23-transfected melanoma cells. Cell 65:25–35
23. Leone A et al (1993) Transfection of human nm23-H1 into the human MDA-MB-435 breast carcinoma cell line: Effects on tumor metastatic potential, colonization, and enzymatic activity. Oncogene 8:2325–2333
24. Parhar RS et al (1995) Effects of cytokine mediated modulation of Nm23 expression on the invasion and metastatic behavior of B16F10 melanoma cells. Int J Cancer 60:204–210
25. Miyazaki H et al (1999) Overexpression of nm23-H2/NDP Kinase B in a human oral squamous cell carcinoma cell line results in reduced metastasis, differentiated phenotype in the metastatic site, and growth factor-independent proliferative activity in culture. ClinCancer Res 5:4301–4307
26. Liu F et al (2002) Transfection of the nm23-H1 gene into human hepatocarcinoma cell line inhibits the expression of sialyl Lewis X, a1,3 fucosyltransferase VII, and metastatic potential. J Cancer Res Clin Oncol 128:189–196
27. Che G et al (2006) Transfection of nm23-H1 increased expression of beta-Catenin, E-cadherin and TIMP-1 and decreased the expression of MMP-2, CD44v6 and VEGF and inhibited the metastatic potential of human non-small cell lung cancer cell line L9981. Neoplasma 53(6):530–537

28. Lim J et al (2011) Cell-permeable NM23 Blocks the maintenance and progression of established pulmonary metastasis. Can Res 71(23):7216–7225
29. Fan Y et al (2013) nm23-H1 gene driven by hTERT promoter induces inhibition of invasive phenotype and metastasis of lung cancer xenograft in mice. Thoracic Cancer 4(1):41–52
30. Jarrett SG et al (2013) NM23 deficiency promotes metastasis in a UV radiation-induced mouse model of human melanoma. Clin Exp Metas 30(1):25–36
31. Yokoyama A et al (1998) Evaluation by multivariate analysis of the differentiation inhibitory factor nm23 as a prognostic factor in acute myelogenous leukemia and application to other hematologic malignancies. Blood 91(6):1845–1851
32. Dearolf C, Hersperger E, Shearn A (1988) Developmental consequences of awdb3, a cell autonomous lethal mutation of Drosophila induced by hybrid dysgenesis. Dev Biol 129:159–168
33. Woolworth JA, Nallamothu G, Hsu T (2009) The drosophila metastasis suppressor gene Nm23 homolog, awd, regulates epithelial integrity during oogenesis. Mol Cell Biol 29(17):4679–4690
34. Dammai V et al (2003) Drosophila awd, the homolog of human nm23, regulates FGF receptor levels and functions synergistically with shi/dynamin during tracheal development. Genes Dev 17(22):2812–2824
35. Ignesti M et al (2014) Notch signaling during development requires the function of awd, the Drosophila homolog of human metastasis suppressor gene Nm23. BMC Biol. https://doi.org/10.1186/1741-7007-12-12
36. Nallamothu G et al (2008) awd, the homolog of metastasis suppressor gene Nm23, regulates Drosophila epithelial cell invasion. Mol Cell Biol 28(6):1964–1973
37. Boissan M et al (2014) Nucleoside diphosphate kinases fuel dynamin superfamily proteins with GTP for membrane remodeling. Science 344(6191):1510–1515
38. Khan I, Gril B, Steeg PS (2019) Metastasis suppressors NME1 and NME2 promote dynamin 2 oligomerization and regulate tumor cell endocytosis, motility, and metastasis. Can Res 79(18):4689–4702
39. Romani P et al (2016) Dynamin controls extracellular level of Awd/Nme1 metastasis suppressor protein. Naunyn-Schmiedebergs Arch Pharmacol 389(11):1171–1182
40. Romani P et al (2018) Extracellular NME proteins: a player or a bystander? Lab Invest 98(2):248–257
41. Bunce CM, Khanim FL (2018) The "known-knowns", and "known-unknowns" of extracellular Nm23-H1/NDPK proteins. Lab Invest 98(5):602–608
42. Ross DT et al (2000) Systematic variation in gene expression patterns in human cancer cell lines. Nat Genet 24(3):227–235
43. Chambers AF (2009) MDA-MB-435 and M14 cell lines: identical but not M14 melanoma? Cancer Res 69(13):5292–5293
44. Horak CE et al (2007) Nm23-H1 suppresses tumor cell motility by down-regulating the lysophosphatidic acid receptor EDG2. Cancer Res 67(15):7238–7246
45. Chevallet M et al (2007) Toward a better analysis of secreted proteins: the example of the myeloid cells secretome. Proteomics 7(11):1757–1770
46. Wortzel I et al (2019) Exosome-mediated metastasis: communication from a distance. Dev Cell 49(3):347–360
47. Babst M et al (2000) Mammalian tumor susceptibility gene 101 (TSG101) and the yeast homologue, Vps23p, both function in late endosomal trafficking. Traffic 1(3):248–258
48. Okabayashi S, Kimura N (2010) LGI3 interacts with flotillin-1 to mediate APP trafficking and exosome formation. NeuroReport 21(9):606–610
49. Ostrowski M et al (2010) Rab27a and Rab27b control different steps of the exosome secretion pathway. Nat Cell Biol 12(1):19–30
50. Yang BY et al (2021) Recent advances in liposome formulations for breast cancer therapeutics. Cell Mol Life Sci 78(13):5225–5243
51. Jung YR et al (2016) Silencing of ST6Gal I enhances colorectal cancer metastasis by down-regulating KAI1 via exosome-mediated exportation and thereby rescues integrin signaling. Carcinogenesis 37(11):1089–1097
52. Okabe-Kado J et al (2009) Extracellular NM23 protein promotes the growth and survival of primary cultured human acute myelogenous leukemia cells. Cancer Sci 100(10):1885–1894
53. Anzinger J, et al (2001) Secretion of a nucleoside diphosphate kinase (Nm23-H2) by cells from human breast, colon, pancreas and lung tumors. 44th Annual Meeting of the Western-Pharmacology-Society, Vancouver, Canada Mar 25–29 Proceedings of the Western Pharmacology Society. Vol.44, pp 61–3
54. Yokdang N et al (2011) A role for nucleotides in support of breast cancer angiogenesis: heterologous receptor signalling. Br J Cancer 104(10):1628–1640
55. Palazzolo G et al (2012) Proteomic analysis of exosome-like vesicles derived from breast cancer cells. Anticancer Res 32(3):847–860
56. Kruger S et al (2014) Molecular characterization of exosome-like vesicles from breast cancer cells. BMC Cancer. https://doi.org/10.1186/1471-2407-14-44
57. Menard JA et al (2016) Metastasis stimulation by hypoxia and acidosis-induced extracellular lipid uptake is mediated by proteoglycan-dependent endocytosis. Cancer Res 76(16):4828–4840
58. Li YJ et al (2020) Hepatic lipids promote liver metastasis. Jci Insight. https://doi.org/10.1172/jci.insight.136215
59. Luo XJ et al (2018) The implications of signaling lipids in cancer metastasis. Exp Mol Med. https://doi.org/10.1038/s12276-018-0150-x
60. Park JW (2002) Liposome-based drug delivery in breast cancer treatment. Breast Cancer Res 4(3):93–97